Article

Chain-Length Heterogeneity Allows for the Assembly of Fatty Acid Vesicles in Dilute Solutions

Itay Budin,[1,2] Noam Prwyes,[1] Na Zhang,[1,3] and Jack W. Szostak[1,*]
[1]Howard Hughes Medical Institute, Department of Molecular Biology and Center for Computational and Integrative Biology, Massachusetts General Hospital, Boston, Massachusetts; [2]Miller Institute for Basic Research in Science, University of California, Berkeley, Berkeley, California; and [3]High Magnetic Field Laboratory, Hefei Institutes of Physical Science, Chinese Academy of Sciences, Hefei, P. R. China

ABSTRACT A requirement for concentrated and chemically homogeneous pools of molecular building blocks would severely restrict plausible scenarios for the origin of life. In the case of membrane self-assembly, models of prebiotic lipid synthesis yield primarily short, single-chain amphiphiles that can form bilayer vesicles only at very high concentrations. These high critical aggregation concentrations (cacs) pose significant obstacles for the self-assembly of single-chain lipid membranes. Here, we examine membrane self-assembly in mixtures of fatty acids with varying chain lengths, an expected feature of any abiotic lipid synthesis. We derive theoretical predictions for the cac of mixtures by adapting thermodynamic models developed for the analogous phenomenon of mixed micelle self-assembly. We then use several complementary methods to characterize aggregation experimentally, and find cac values in close agreement with our theoretical predictions. These measurements establish that the cac of fatty acid mixtures is dramatically lowered by minor fractions of long-chain species, thereby providing a plausible route for protocell membrane assembly. Using an NMR-based approach to monitor aggregation of isotopically labeled samples, we demonstrate the incorporation of individual components into mixed vesicles. These experiments suggest that vesicles assembled in dilute, mixed solutions are depleted of the shorter-chain-length lipid species, a finding that carries implications for the composition of primitive cell membranes.

INTRODUCTION

Because of their prebiotic plausibility and ability to spontaneously assemble into vesicles, fatty acids have long been proposed to serve a role as early cell membrane lipids (1,2). Experimental models for abiotic lipid synthesis include high-temperature, high-pressure Fischer Tropsch-type chemistry (3) and spark-discharge reactions (4), both of which yield mixtures of fatty acids, fatty alcohols, and alkanes. The most abundant amphiphilic species in these mixtures are short, saturated fatty acids (<C12), which are also the primary species found in carbonaceous chondrite extracts (5). Longer-chain products (>C14) are also detected, but in decreasing abundance with chain length, as would be expected from a nonenzymatic condensation process. Fatty acids assemble into bilayer membranes only when the solution pH is near the pKa of the bilayer-associated acid (~7–9 depending on the chain length (6)). This condition allows for approximately equal proportions of protonated and ionized carboxylate headgroups, thereby minimizing charge repulsion and providing a stabilizing hydrogen-bond network (6,7). Higher- or lower-pH solutions favor the formation of micelles or oil droplets, respectively, upon aggregation.

Although studies of fatty acid membranes, including this one, do not necessarily mimic prebiotic conditions, they are useful for characterizing the properties and dynamics of these complex systems in defined laboratory conditions. Vesicles composed of short-chain fatty acids and related monoacyl lipids have been shown to exhibit several physicochemical properties that make them well suited for a role as primitive cell compartments. For example, short- and medium-chain fatty acid membranes ($\leq$C14) feature high intrinsic solute permeability, which is a requirement for a primitive cell that depends on nonfacilitated membrane transport (8). Membrane growth and division have also been demonstrated via several pathways (2,9,10), all of which depend on the aqueous solubility of fatty acids for their incorporation into preformed vesicles. However, this intrinsic solubility also provides a thermodynamic barrier against membrane assembly: fatty acids are characterized by significant critical aggregation concentrations (cacs), and aggregation into membrane vesicles only occurs above the cac. Critical concentrations are a result of the entropic cost of molecular association into large aggregates and are analogous to saturation concentrations for solubility. They are therefore modeled as phase separations, in which the cac represents the concentration at which the favorable energy of aggregation offsets the statistical entropic cost of remaining in solution. Therefore,

$$\mu_a^\circ - \mu_w^\circ = RT \ln cac \quad (1)$$

Submitted February 6, 2014, and accepted for publication July 30, 2014.

*Correspondence: szostak@molbio.mgh.harvard.edu

Editor: Tobias Baumgart.

0006-3495/14/10/1582/9 $2.00

http://dx.doi.org/10.1016/j.bpj.2014.07.067

where μ_a° and μ_w° are the standard free energies of an amphiphile in an aggregate and as a monomer in water, respectively, and the cac is expressed as a unitless mole fraction of the system (i.e., the usual cac, expressed as a molar concentration, divided by ~55 M). Because the free energy of aggregation via the hydrophobic effect increases linearly by a proportionality constant (k) with chain length (nCH_2),

$$cac = e^{\frac{\mu_a^\circ - \mu_w^\circ}{RT}} \propto e^{\frac{-k(nCH_2)}{RT}} \quad (2)$$

As a result, the cac values tend to increase exponentially with decreasing chain length (Fig. 1). Thus, whereas long-chain fatty acids assemble at reasonable concentrations (e.g., oleic acid (OA): C18:1, 20 μM), short-chain species require very high concentrations (e.g., decanoic acid (DA): C10, 40 mM; octanoic acid: C8, 250 mM). Since shorter-chain fatty acids are likely to be the abiotically more abundant than long-chain fatty acids, these concentration requirements pose a potential hurdle for the assembly of primitive cells. The high melting temperatures of saturated long-chain fatty acids (e.g., stearic acid: C18, 70°C) also limit their potential role as primary membrane components in mesophilic conditions as they form waxes or solids. Acyl branching or incorporation of *cis* double bonds, which dramatically lower melting temperatures by disrupting acyl-chain packing, result from enzymatic synthesis and thus are evolved features of lipid structures.

The concentration problem for molecular self-assembly and nonenzymatic chemistry is a long-standing challenge for origin-of-life scenarios. Solvent-phase transitions, such as evaporation and eutectic freezing, have most commonly been proposed as physical mechanisms for overcoming prebiotic concentration barriers. Such concentration processes act on solutes indiscriminately and this is problematic for fatty acids, which precipitate in moderate divalent (>5 mM) or high monovalent (>300 mM) cation concentrations. Processes that concentrate solutes more specifically, such as thermal diffusion columns (11), necessitate very particular and rare microenvironments, and thus are of debatable prebiotic relevance. We hypothesized that the heterogeneity intrinsic to abiotic chemistry could provide a more general solution to the concentration problem for membrane assembly. If small fractions of long-chain species could nucleate vesicle assembly or otherwise lower its entropic barrier, fatty acid mixtures could assemble at lower concentrations than would be expected from their mean chain length.

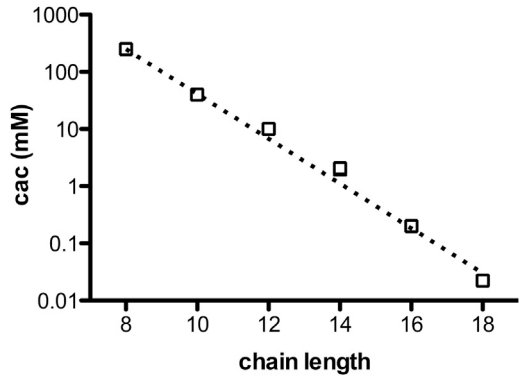

FIGURE 1 Exponential dependence of fatty acid cac on chain length. Cac values were derived from light-scattering measurements and confirmed with pinacyanol chloride. The dashed line is the least-squares fit to Eq. 2, yielding a value for k of -2.3 kJ/mol/CH_2. Measurements were taken in POPSO buffer at 30°C. Due to the high melting temperature of saturated fatty acids, 9-*cis* monounsaturated fatty acids were used for C14, C16, and C18 vesicles, and C12 vesicles were preincubated at 45°C.

Mixtures of single-chain lipids with variable headgroups have previously been shown to exhibit increased thermostability (12), permeability (8), and lower aggregation concentrations (13). However, the properties of fatty acid membranes with acyl-chain polydispersity have not been explored, with the notable exception of narrow mixtures of very short-chain fatty acids (14). We recently (15) showed that fatty acid membrane assembly largely follows the pseudophase transition characteristic of micellar assembly, which is characterized by a largely constant concentration of monomers with increasing total concentration above the cac. Early studies developed aggregation models for mixed surfactant micelles, which have significant practical and commercial value and have been extensively verified experimentally (16–20). These models predict that the cac of a mixture can be described as a weighted average of the reciprocal cac (1/cac) of their individual components and is therefore heavily weighted by long-chain species in the mixture. Here, using several spectroscopic techniques to experimentally characterize the formation of vesicles from fatty acid mixtures, we show that mixed-vesicle assembly behaves similarly.

MATERIALS AND METHODS

Sample preparations

All unlabeled fatty acids were obtained from Nu-Check (Elysian, MN). 1-^{13}C DA, 1-^{13}C OA, and 2-^{13}C glycerol were obtained from Cambridge Isotope Laboratories (Tewksbury, MA). All other reagents were obtained from Sigma-Aldrich (St. Louis, MO). Solutions were prepared by addition of the fatty acids as oils into solutions of Good's buffers (0.2 M Bicine pH 8.5 or 0.1 M POPSO pH 8.2, each titrated with NaOH before addition of lipids), which are commonly used for fatty acid vesicle studies. Concentrated solutions were allowed to equilibrate overnight under gentle agitation, and serial dilutions of these solutions were allowed to equilibrate a further ~12 h. The final pH of the solutions did not necessarily reflect the buffer pH, as additional fatty acid mildly acidified the solutions (Fig. S1 in the Supporting Material), although this effect was small (<0.2 pH units) for fatty acid concentrations within the range of mixed cacs tested (<50 mM). For mixtures containing short-chain lipids, the POPSO buffer provided more abundant vesicle solutions than the Bicine buffer, though it did not dramatically affect the cac (Fig. S2). The mechanism for this effect is unclear but is consistent with the higher encapsulation efficiencies we have observed for short-chain vesicles using this buffer. For spectroscopic cac determination, pinacyanol chloride was added to heated buffered samples to a final concentration of 25 μM and allowed to incubate for >15 min before analysis.

Measurements

Light-scattering intensities were recorded on a PD2000 dynamic light-scattering instrument (Precision Detectors, Bellingham, MA) or a DynaPro plate reader (Wyatt, Santa Barbara, CA). Absorbance readings were taken on a Spectramax 384 plate reader (Molecular Devices, Sunnyvale, CA). Surface tension measurements were taken according to the Noüy ring method using a surface tensiometer (Model 21; Fisher Scientific, Hampton, NH). NMR experiments were performed on a Varian (Agilent, Santa Clara, CA) 400 MHz (^{13}C, 100 MHz) spectrometer (Oxford AS-400) equipped with a Varian 5 mm broadband PFG (z gradient) probe. One-dimensional ^{13}C spectra were recorded with inverse-gated ^{1}H decoupling and a long relaxation delay of 40 s. The linewidth was measured as the half-peak height of a single-function Lorentzian fit via iNMR (Molfetta, Italy). For broad peaks, acquisitions were integrated for 6–12 h to minimize noise. The absence of linewidth artifacts relating to measurement conditions (most notably magnet shimming) was monitored and normalized by including a noninteracting internal standard, 2-^{13}C-gylcerol, at 10 mM in all samples. Glycerol at this concentration did not noticeably affect DA vesicle abundance or the cac in spectroscopic experiments (Fig. S3).

Microscopy

Micrographs were taken on a TE2000-S inverted microscope (Nikon, Tokyo, Japan) with 100× oil objective. Samples were prestained with Rhodamine 6G at 1 μM to visualize membranes. A PE100 temperature-controlled microscope stage (Linkam, Tadworth, UK) was used to maintain a temperature of 30°C. To prevent high-melting-point, long-chain lipids from crystallizing out of solution, the slides were preheated on the stage before addition of the sample.

RESULTS

The phase behavior of multicomponent surfactant systems has been studied extensively in the context of the critical micelle concentrations of surfactant mixtures. Assuming a phase-separation model of aggregation, the cac of a mixture can be derived (Supporting Material) as a function of the individual cacs of the components and their mole fractions in the mixture:

$$\frac{1}{cac} = \sum_{i=1}^{k} \frac{X_i}{f_i cac_i} \tag{3}$$

where cac is the mixed cac for the system (expressed as the mole fraction of the total system, e.g., molar concentrations divided by 55 M) with k components, each with mole fractions X_i, individual critical concentrations cac_i for their behavior in single-component systems, and activity coefficient f_i. For micelles, fatty acids have shown ideal behavior (19), i.e., an activity coefficient of one, thus potentially simplifying this further. For a binary, ideal system, Eq. 3 reduces to

$$cac = \frac{cac_1 cac_2}{X_1 cac_2 + (1 - X_1) cac_1} \tag{4}$$

In this expression, the cac of the mixture approaches the lower of the two individual cacs as their ratio (cac_2/cac_1) rises (for example values, see Fig. S4). We therefore hypothesized that in mixtures with a wide range of chain lengths, longer-chain lipids, with correspondingly lower individual cacs, largely determine the net cac of the system.

To experimentally test this model, we first characterized a binary mixture of monounsaturated fatty acids: myristoleic acid (MA, C14:1, cac 2 mM) and OA (C18:1, cac 20 μM). We measured critical concentrations by monitoring the light-scattering intensities of serial dilutions, in which the presence of assembled vesicles results in a sudden increase in intensity per unit concentration above the cac (Fig. 2 *A*). This is because vesicles are much larger (~100 nm to several micrometers) than micelles or monomers and scattering scales nonlinearly with particle diameter; therefore, the measured intensity increases dramatically upon vesicle formation relative to the pre-cac concentration. The measured cac values (Fig. 2 *B*) for this binary mixture matched those predicted by theory well, with 10% OA decreasing the cac of myristoleate to 125 μM, an almost 20-fold reduction. Surface-tension measurements on serial dilutions of this mixture (Fig. S5) showed a single plateau, consistent with a single critical concentration. The

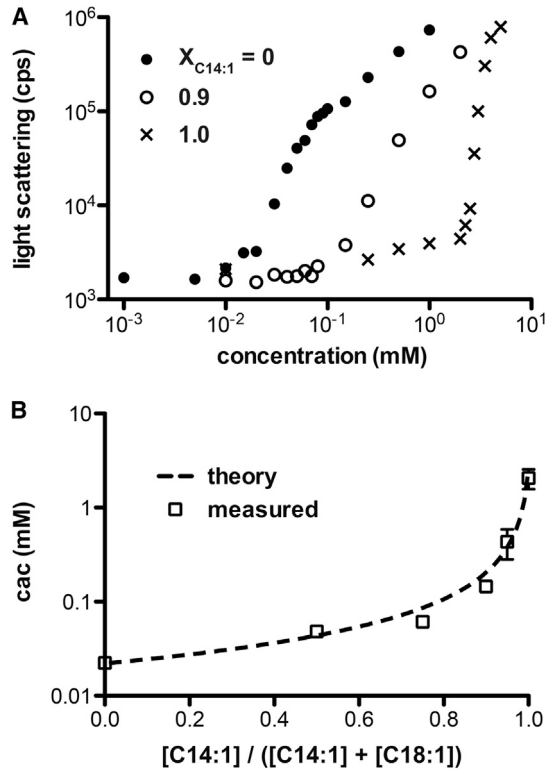

FIGURE 2 Cacs for binary mixtures of MA (C14:1) and OA (C18:1). (*A*) Light-scattering intensities show a single concentration-dependent aggregation transition for MA, OA, and a 90:10 mixture of the two at 2 mM, 20 μM, and 100 μM, respectively. Measurements were taken from serial dilutions of each sample at room temperature; the sudden increase in light scattering results from the assembly of vesicle aggregates and takes place at the cac. (*B*) Cac, as measured by light scattering, as a function of MA fraction. Samples were prepared in Bicine buffer at 23°C. Error bars indicate ± standard deviation (SD; n = 3); nonvisible error bars indicate a small SD relative to the symbol marker. Predicted values were calculated from ideal theory using Eq. 4.

concentration at which added lipid ceased to retard surface tension was at or above that of the cac as measured by light scattering, indicating the absence of aggregation (e.g., of micelles) in more dilute solutions.

Encouraged by these results, we tested more prebiotically relevant mixtures using a short-chain, saturated lipid, DA (C10:0, cac 40 mM). Mixtures of DA with medium- and long-chain fatty acids did not consistently show sharp discontinuities in light-scattering intensities. We hypothesized that this was a result of a low partition coefficient of the short-chain species into mixed vesicles in concentrations near the cac, due to both statistical effects inherent to mixed systems (discussed further below) and the presence of nonscattering micelle aggregates (15). Such concentration-dependent aggregation partitions obscure sharp transitions in scattering because the abundance of vesicles is low in solutions just above the cac (e.g., see Fig. 5 *A* in Budin et al. (15)). Therefore, we instead used the spectroscopic probe pinacyanol chloride, a cyanine dye that undergoes a dramatic colorimetric change in the presence of hydrophobic aggregates (21), to monitor vesicle assembly. Solutions containing low concentrations of pinacyanol (25 μM) turn from a clear purple to a strong blue in the presence of aggregates, which one can see visually or by measuring the solution's absorbance at 610 nm vs. 530 nm (Fig. 3). This change is a result of the dependence of the hydrophobic dye's self-aggregation on the polarity of its solvent environment (22). Therefore, this assay does not distinguish between different types of aggregate (e.g., micelle or vesicle)—it only discerns whether a hydrophobic microenvironment is present. We previously showed that fatty acid vesicle solutions feature only a single cac, above which aggregation results in an equilibrium mixture of vesicles and micelles that is dependent on pH and concentration (15). Using this method, we measured the cac of DA/MA (C14:1) mixtures, which matched predicted values (Fig. 4 *A*). The saturated myristic acid (C14) had a quantitatively similar effect on DA mixtures compared with its unsaturated analog, even though it was unable to form vesicles independently at 30°C because of its high melting temperature (~55°C). Thus, the ability of short-chain, low-melting-temperature fatty acids to solubilize long-chain fatty acids below their melting temperature is a viable mechanism for reducing aggregation concentrations. Finally, we measured the cac of DA in binary mixtures with 10% fatty acids of varying chain lengths (Fig. 4 *B*). Our ideal model fit the measured values well, although there was a deviation from the model for the long-chain-length fatty acids tested (C16:1 and C18:1). The effect of these long-chain fatty acids on cac was still substantial; for example, compared with pure DA, 10% C16:1 yielded a 15-fold reduction in cac, and 10% C18:1 yielded a 100-fold reduction in cac.

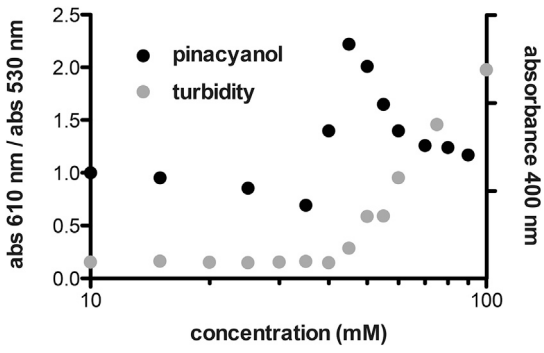

FIGURE 3 Vesicle assembly monitored by a colorimetric assay. Serial dilutions of DA were incubated with 25 μM pinacyanol chloride. The sudden increase in the red-to-green absorption ratio (*black*, left axis) at the cac (40 mM) indicates the presence of pinacyanol monomers, which are only solubilized in the presence of hydrophobic microenvironments (e.g., micelles or bilayers). This absorbance ratio falls back close to one at high concentrations due to the turbidity of the vesicle solution, which drowns out the dye absorbance. The turbidity (as a measure of light scattering) of identical samples without dye (*gray*, right axis) shows a matching cac at 40 mM. Samples were prepared in POPSO buffer at 30°C.

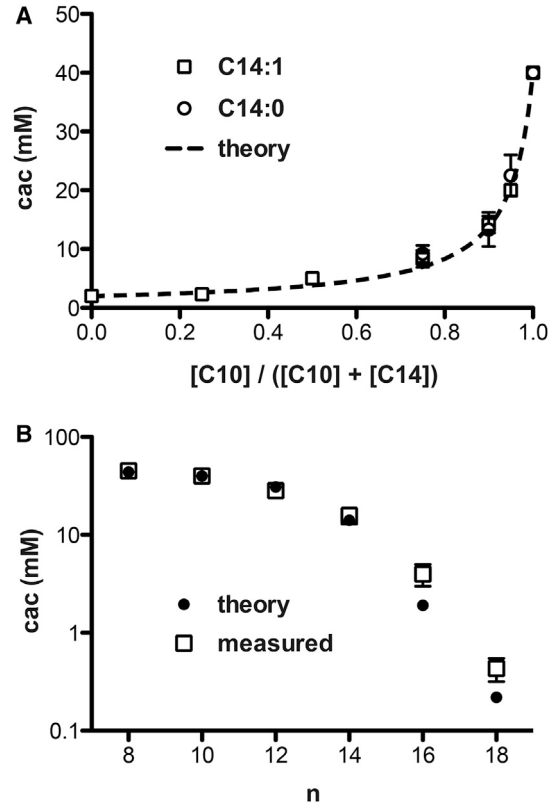

FIGURE 4 Cacs for binary mixtures with DA (C10). (*A*) Cac values for DA and either MA (C14:1) or myristic acid (C14:0) as a function of DA fraction. Myristic acid notably lowers the cac despite the inability of pure myristic acid to form vesicles at this temperature (30°C). (*B*) Cac for DA with 10 mol % of the given chain length fatty acid. The minor component was saturated for $n = 8$, 10, and 12, and unsaturated for $n = 14$, 16, and 18. Samples were prepared in POPSO buffer at 30°C and cac values were measured using pinacyanol chloride. Error bars indicate ± SD ($n = 3$); nonvisible error bars indicate a small SD relative to the symbol marker. Predicted values were calculated from theory using Eq. 4.

We next tested whether our model predicts the cac of multicomponent fatty acid mixtures. We measured the cac of a series of ternary mixtures containing DA, MA, and octanoic acid using pinacyanol chloride (Fig. 5). We kept the ratio of the MA to octanoic acid at 1:2 while varying the DA content in the mixture. The mean chain length in this series thus remained constant ($n = 10$) whereas the chain-length variance of the mixture increased with decreasing DA content. The resulting cac values followed the ideal mixing model, demonstrating that fatty acid mixtures can allow for vesicle assembly at much lower concentrations (here, ~5-fold) than single-component solutions with the same average chain length. Because of its lower pKa compared with longer-chain lipids, pure octanoic acid does not form vesicles at the pH of these solutions (>8.0) (23), but this did not lead to a significant deviation from the ideal mixing model.

Our spectroscopic data show that minor fractions of long-chain fatty acids can dramatically lower the concentration barrier for assembly of primarily short-chain mixtures. We confirmed this by fluorescence microscopy of DA mixtures using the membrane stain Rhodamine 6G. In the case of a 95:5 DA/MA solution, small vesicles were observed at 25 mM, above the measured cac of 20 mM (Fig. 6 *A*). Vesicle assembly in this case is strictly cooperative, as neither component assembles into visible structures at its respective concentration in the mixture. In the case of a 95:5 DA/OA mixture (measured cac of 0.5 mM), we observed dense fields of vesicles at 15 mM (Fig. 6 *B*), a concentration at which pure DA fails to assemble into vesicles. Pure OA at its respective concentration in the mixture (0.75 mM) supports vesicle assembly because of its low cac, but produces only sparse fields of small, suboptical vesicles. Since very dilute solutions generally feature small vesicle sizes in fatty acid systems (e.g., see Fig. S4 in Budin et al. (24)), this observation is consistent with substantial incorporation of the short-chain species into the membranes, thus allowing for an increased abundance of vesicles. Our recent models for protocell division (9) depend on the presence of large vesicles (approximately micrometers in size), and thus vesicle abundance and size are important considerations for protocell assembly.

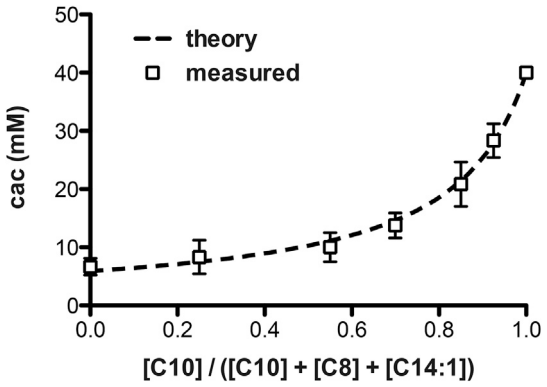

FIGURE 5 Cacs for a ternary mixture of DA, octanoic acid, and MA. The ratio of octanoic acid to MA was kept at 2:1, with their sum equal to $1 - X_{C10}$. The mean chain length of the mixtures is thus constant at $n = 10$ throughout this range. Samples were prepared in POPSO buffer at 30°C and measurements were taken using pinacyanol chloride. Error bars indicate ± SD ($n = 3$); nonvisible error bars indicate a small SD relative to the symbol marker. Theoretical values were calculated using Eq. 3.

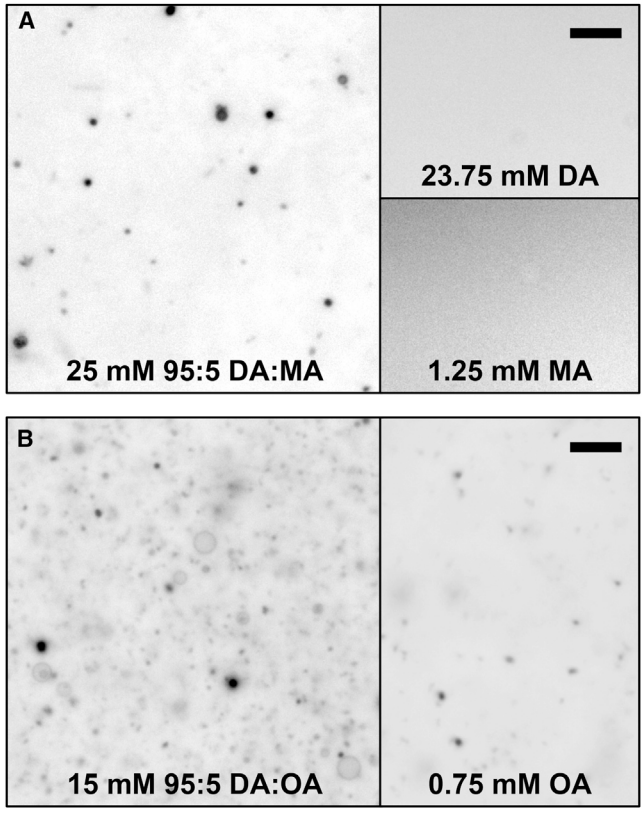

FIGURE 6 Micrographs demonstrating the effects of fatty acid mixtures on vesicle assembly. (*A*) A binary mixture of 95:5 DA (C10)/MA (C14:1) assembles into visible vesicles at 25 mM (23.75 mM DA, 1.25 mM MA), above its cac of 20 mM. The individual fatty acids (*right panels*) do not assemble at their respective concentrations. (*B*) A binary mixture of 95:5 DA/OA (C18:1) produces large, plentiful vesicles at 15 mM. The OA component (5 mol %) lowers the cac of the DA from 40 mM to 500 μM. OA can still assemble into vesicles at its respective concentration (0.75 mM), but the resulting vesicles are small and in low abundance because of the low net concentration of fatty acids. All samples were prepared in POPSO buffer, labeled with the membrane stain Rhodamine 6G, and imaged at 30°C. Scale bar, 6 μm.

These experiments motivated us to directly probe the composition of the resulting mixed vesicles. Do mixtures allow predominantly short-chain lipid vesicles to assemble in dilute solutions? Or are the resulting vesicles simply the minor, long-chain species undergoing a phase separation? Answering these questions requires techniques to monitor the aggregation states of multiple fatty acid components in a mixture. The methods described above, however, can only discern the presence of aggregates, not their composition. Furthermore, the fast dynamics of fatty acid

systems (exchange times of well under a second; see Fig. S3 in Budin and Szostak (10)) preclude the use of any physical separation. Our laboratory previously probed fatty acid dynamics with NMR (25), and a common challenge in such experiments is the dramatic resonance (peak) broadening that accompanies the association of lipids with large vesicles, which are characterized by slow tumbling times and anisotropic motions of associated lipids within the bilayer. Here, we took advantage of this phenomenon by using the linewidth as a readout of the aggregation state (Fig. 7). Fatty acids labeled with ^{13}C at the carbonyl group are commercially available and provide distinct, single peaks at ~180 ppm of one-dimensional ^{13}C spectra. Below the cac or under conditions that do not allow for membrane assembly (such as at high pH), ^{13}C DA exhibits a sharp peak consistent with monomers in solution (Fig. 7 *A*). Above the cac, linewidth increases with concentration and corresponds well with the turbidity of the solution (*inset*). Because short-chain fatty acids exchange very rapidly between coexisting phases (aggregates and monomers), we interpret this line broadening as reflecting a weighted average of the monomers and aggregates in the solution. Within the concentration ranges tested, the measured DA linewidths are consistent with that model (Supporting Material).

Although assessing the NMR linewidth is not a convenient or sensitive approach for measuring cac, it can allow one to discern the aggregation state of individual labeled components in a mixture of otherwise unlabeled species. We therefore used this approach to analyze mixtures of DA and OA by isotopically labeling the individual fatty acid species and monitoring their peak broadening as a result of changes in their concentration and stoichiometry. At 15 mM, a concentration below its cac of 40 mM, DA exhibits a sharp peak, reflecting an absence of vesicles. Upon addition of unlabeled 5% OA, the ^{13}C DA peak showed significant broadening, indicating at least a partial partition of the DA into mixed vesicles (final concentrations: 0.75 mM OA and 14.25 mM DA, as in Fig. 6 *B*). Peak broadening further increased when the total lipid concentration was increased to 50 mM or when the OA fraction was increased to 50% (Table 1). When we repeated these experiments with 1-^{13}C OA and unlabeled DA, we did not observe these changes in linewidth (see spectra in Supporting Material). Instead, OA exhibited universally very broad peaks (>100 Hz) irrespective of the solution concentration (15 or 50 mM) or composition (0%, 50%, or 95% DA). We interpret these results as reflecting the varying vesicle partition of DA as a function of concentration with respect to the mixed cac of the system (e.g., DA is depleted from vesicles in dilute solutions). In contrast, OA features a high partition into the mixed vesicles in this concentration regime, which is expected due to its ~1000-fold lower individual solubility. This characterization is consistent with previous models (16) and experiments (26) on mixed micelles (discussed further below), in which the micelle or monomer composition in dilute solutions was found to deviate from the total component stoichiometry.

DISCUSSION

The chemical heterogeneity that is intrinsic to abiotic chemistry is a fundamental consideration in models for the origin

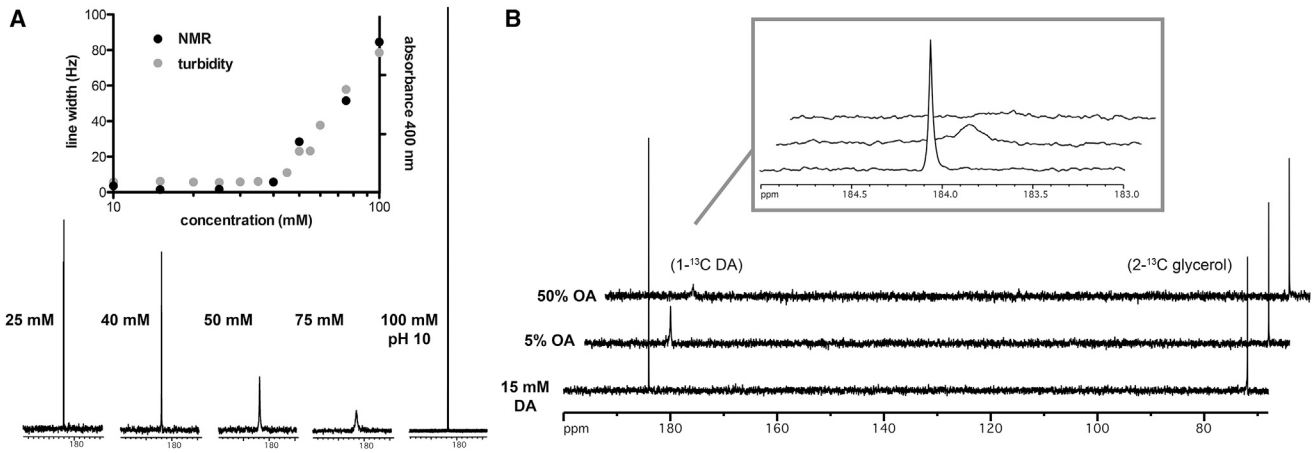

FIGURE 7 Aggregation detected by changes in the one-dimensional ^{13}C NMR linewidth of 1-^{13}C DA. The slow tumbling of vesicle aggregates causes the broadening of peaks associated with membrane-partitioned lipids, allowing the peak width to be a measurement of the vesicle partition of the labeled species. (*A*) Spectra show the characteristic peak (184 ppm) for increasing concentrations of DA. Peak broadening occurs in samples above the DA cac of 40 mM. Preventing vesicle formation by raising the solution pH to 10 removes this line broadening. The resulting linewidths (*inset*) start to increase at the cac. Turbidity data for DA are superimposed (*gray*, right axis) to show agreement with the NMR measurements. Full spectra are available in the Supporting Material. (*B*) Addition of OA (C18:1) as a minor component (5%) drives the incorporation of DA (C10) into vesicles at a concentration of 15 mM, below its individual cac. This is monitored by the broadening of the narrow characteristic peak from 1.5 Hz, consistent with a purely monomer phase, to 16 Hz. Further incorporation of OA (50%) causes increased broadening (36 Hz). 2-^{13}C glycerol (71 ppm) is included as an internal standard and features a constant linewidth (1.08 Hz, SD = 0.03). Measurements were made in POPSO buffer at 30°C; linewidths were taken at half-peak height.

TABLE 1 Linewidths of 1-^{13}C DA in the given mixtures

15 mM ^{13}C DA	50 mM ^{13}C DA	15 mM 95:5 1-^{13}C DA/OA	50 mM 95:5 1-^{13}C DA/OA	15 mM 50:50 1-^{13}C DA/OA
1.6 ± 0.6 Hz	28.6 ± 5.6 Hz	14.2 ± 3.3 Hz	49.1 ± 7.0 Hz	36.3 ± 2.9 Hz

Values are given as ± SD (n = 3). Peak broadening at 15 mM in the presence of 5% OA was statistically significant ($p = 0.0001$, by a paired *t*-test), as was further broadening at 50 mM ($p = 0.003$) or 50% OA ($p = 0.008$). All samples were prepared in POPSO buffer at 30°C. Spectra are available in the Supporting Material. DA, decanoic acid; OA, oleic acid.

of life (27,28). Here, we have shown that mixtures of fatty acids of varying chain lengths self-assemble into membranes at significantly lower concentrations than would be expected based on their primary components. Although the cac values we report are specific to the laboratory conditions chosen here, especially in regard to pH, buffer, and temperature, these findings provide a useful framework for predicting the conditions needed for primitive membrane assembly. Our consideration of the assembly of membranes from mixtures of different-chain-length fatty acids was motivated by extensive theoretical and experimental work on mixed surfactant micelles. We have shown that the ideal mixing models developed for those systems apply to mixed fatty acid vesicles as well, and predict a nonlinear (reciprocal) dependence of mixed cac on the cac of each component in the mixture. Laboratory simulations of fatty acid synthesis yield product distributions that decrease in quantity with chain length, but still feature significant fractions of longer-chain-length lipids (3,4). Characterizing the aggregation of such product mixtures would therefore allow one to estimate the lipid concentrations necessary for prebiotic membrane assembly.

Other potential barriers to prebiotic membrane self-assembly remain, however, especially the rather narrow range of acceptable chemical environments regarding solution pH and salt concentration. Fatty acid-based membranes remain fundamentally incompatible with acidic or very basic solutions: aggregation due to the hydrophobic effect still occurs, but as oil droplets or micelles, respectively. Only a narrow span of pH values allows for vesicle assembly, and this range is itself dependent on chain length, with short-chain fatty acids requiring solutions closer to neutral. This effect could explain the slight deviations from the ideal cac model we observed for mixtures of long-chain-length fatty acids ($n > 14$) with DA (Fig. 4 *B*). An interesting possibility is that changes in pH could influence the cac and vesicle composition of fatty acid mixtures by altering the components that participate in aggregation and their individual cac values. The incorporation of hydrogen-bonding lipid species, glycerol monoesters (13), or fatty alcohols (23) has been shown to loosen this pH restriction, and fatty alcohols in particular are an abundant by-product of fatty acid synthesis by Fischer Tropsch-type chemistry (3). These membrane components also increase the tolerance of fatty acid vesicles to salts (29), as does the addition of partial chelating agents, such as citrate (30), to the solution.

Vesicle assembly from a mixture of fatty acids that has reached its mixed cac does not imply that the composition of the resulting vesicles will reflect that of the solution as a whole. The ideal mixed-micelle model used here for cac calculations has been extended to the composition of mixed aggregates (16) and predicts that aggregates in dilute solutions will be depleted in the short-chain, more soluble species. In single-component fatty acid systems, aggregation follows a pseudophase model and therefore features two concentration regimes: 1), below the cac, a purely monomer phase with a concentration equal to the total concentration; and 2), above the cac, a constant concentration of monomers and an increasing concentration of aggregates, including micelles and vesicles. In mixed systems, there is an additional concentration regime in between the mixed cac and the cac of the shortest-chain component, in which aggregate abundance increases nonlinearly with concentration because the monomer-vesicle partition coefficients are themselves concentration dependent. Therefore, the vesicle partition of an individual fatty acid species is expected to be concentration dependent below its individual cac. In the very few cases in which investigators have been able to obtain compositional measurements, such as by extrapolating the conductivities of anionic surfactant mixtures (25), the experimental data have matched this model. In a complex mixture of different-chain-length species, as would be expected from prebiotic chemistry, a regime of variable membrane composition could be dominant throughout the relevant concentration range, as even trace amounts of very-long-chain fatty acid lead to low critical concentrations. Thus, a major aim of future work will be to quantitatively characterize vesicle composition in fatty acid mixtures as a function of both component stoichiometry and concentration, and evaluate how closely the actual vesicle composition obeys the ideal mixed-component vesicle model. The NMR approach used here to establish DA participation in aggregates is a potential strategy for obtaining such measurements by modeling the measured linewidths as the weighted average of states and extrapolating the partition coefficients:

$$lw = X_m lw_m + X_a lw_a \tag{5}$$

where lw is the measured linewidth of the sample, X_m is the fraction of fatty acid molecules that are monomers, lw_m is the linewidth for a pure monomer sample, X_a is the fraction of fatty acid molecules that are in vesicle aggregates, and

lw_a is the linewidth for a pure vesicle aggregate fraction. By approximating the vesicle linewidth as constant in our experiments (see Fig. S6, and Table S1 in the Supporting Material for calculation and explanation), we estimated that the 95:5 DA/OA mixture in Table 1 featured a 4-fold higher partition of DA into vesicles as the total concentration increased from 15 to 50 mM.

Acyl-chain length is the key determinant of membrane properties in fatty acid membranes and therefore is an important consideration in models of primitive cell function. For example, membranes composed of short-chain lipids are more permeable to chemical building blocks (8), but are also more prone to high-temperature leakage (12). Therefore, the thermodynamics of vesicle assembly from fatty acid mixtures could carry important implications for the functional properties of primitive cell membranes. Vesicles composed of short, single-chain lipid membranes, which are generally regarded as prebiotic models, might not best mimic membranes formed by mixtures in dilute solutions if dilute aggregates are enriched in longer-chain species. Relevant processes that alter total lipid concentration, such as solution evaporation and de novo lipid synthesis, could also potentially modulate membrane compositions and related functional properties. Such compositional dynamics may allow for phenomena that are advantageous for primitive cell models, for example, by triggering a switch to more permeable membranes during periods of increased concentrations of surrounding chemical building blocks.

CONCLUSIONS

We have provided a quantitative description of the assembly of vesicles from mixtures of fatty acids with varying chain length, which serves as a model for membrane formation from abiotically derived building blocks during the origin of life. Theoretical models and experimental measurements of cacs from such systems demonstrate that the cac is largely determined by long-chain species in the mixture even when they are included as small molar fractions. Therefore, small amounts of long-chain lipids can allow for the assembly of single-chain vesicles in dilute environments with primarily short-chain components. Experiments analyzing the resulting vesicles suggest that the the composition of such membranes is a function of both the solution stoichiometry and concentration.

SUPPORTING MATERIAL

Six figures, one table, supplemental information, and supporting references are available at http://www.biophysj.org/biophysj/supplemental/S0006-3495(14)00838-8.

The authors thank Anik Debnath and Raphael Bruckner for helpful discussions.

This research was supported in part by grant EXB02-0031-0018 from the NASA Exobiology Program to J.W.S. I.B. is a fellow at the Miller Institute for Basic Science. J.W.S. is an investigator of the Howard Hughes Medical Institute.

REFERENCES

1. Hargreaves, W. R., and D. W. Deamer. 1978. Liposomes from ionic, single-chain amphiphiles. *Biochemistry.* 17:3759–3768.
2. Hanczyc, M. M., S. M. Fujikawa, and J. W. Szostak. 2003. Experimental models of primitive cellular compartments: encapsulation, growth, and division. *Science.* 302:618–622.
3. Simoneit, B. R. T. 2004. Prebiotic organic synthesis under hydrothermal conditions: an overview. *Adv. Space Res.* 33:88–94.
4. Yuen, G. U., J. G. Lawless, and E. H. Edelson. 1981. Quantification of monocarboxylic acids from a spark discharge synthesis. *J. Mol. Evol.* 17:43–47.
5. Yuen, G. U., and K. A. Kvenvolden. 1973. Monocarboxylic ccids in Murray and Murchison carbonaceous meteorites. *Nature.* 246: 301–303.
6. Cistola, D. P., J. A. Hamilton, …, D. M. Small. 1988. Ionization and phase behavior of fatty acids in water: application of the Gibbs phase rule. *Biochemistry.* 27:1881–1888.
7. Cistola, D. P., D. Atkinson, …, D. M. Small. 1986. Phase behavior and bilayer properties of fatty acids: hydrated 1:1 acid-soaps. *Biochemistry.* 25:2804–2812.
8. Mansy, S. S., J. P. Schrum, …, J. W. Szostak. 2008. Template-directed synthesis of a genetic polymer in a model protocell. *Nature.* 454: 122–125.
9. Zhu, T. F., and J. W. Szostak. 2009. Coupled growth and division of model protocell membranes. *J. Am. Chem. Soc.* 131:5705–5713.
10. Budin, I., and J. W. Szostak. 2011. Physical effects underlying the transition from primitive to modern cell membranes. *Proc. Natl. Acad. Sci. USA.* 108:5249–5254.
11. Duhr, S., and D. Braun. 2006. Why molecules move along a temperature gradient. *Proc. Natl. Acad. Sci. USA.* 103:19678–19682.
12. Mansy, S. S., and J. W. Szostak. 2008. Thermostability of model protocell membranes. *Proc. Natl. Acad. Sci. USA.* 105:13351–13355.
13. Maurer, S. E., D. W. Deamer, …, P. A. Monnard. 2009. Chemical evolution of amphiphiles: glycerol monoacyl derivatives stabilize plausible prebiotic membranes. *Astrobiology.* 9:979–987.
14. Cape, J. L., P.-A. Monnard, and J. M. Boncella. 2011. Prebiotically relevant mixed fatty acid vesicles support anionic solute encapsulation and photochemically catalyzed trans-membrane charge transport. *Chem. Sci.* 2:661–671.
15. Budin, I., A. Debnath, and J. W. Szostak. 2012. Concentration-driven growth of model protocell membranes. *J. Am. Chem. Soc.* 134:20812–20819.
16. Clint, J. H. 1975. Micellization of mixed nonionic surface active agents. *J. Chem. Soc. Faraday Trans.* 71:1327–1334.
17. Clint, J. H. 1992. Surfactant Aggregation. Blackie, Glasgow/London.
18. Motomura, K., M. Yamanaka, and M. Aratono. 1984. Thermodynamic consideration of the mixed micelle of surfactants. *Colloid Polym. Sci.* 262:948–955.
19. Shinoda, K. 1954. The critical micelle concentration of soap mixtures (two-component mixture). *J. Phys. Chem.* 58:541–544.
20. Holland, P. M., and D. N. Rubingh. 1983. Nonideal multicomponent mixed micelle model. *J. Phys. Chem.* 87:1984–1990.
21. Corrin, M. L., and W. D. Harkins. 1947. Determination of the critical concentration for micelle formation in solutions of colloidal electrolytes by the spectral change of a dye. *J. Am. Chem. Soc.* 69:679–683.
22. West, W., and S. Pearce. 1965. The dimeric state of cyanine dyes. *J. Phys. Chem.* 69:1894–1903.

23. Apel, C. L., D. W. Deamer, and M. N. Mautner. 2002. Self-assembled vesicles of monocarboxylic acids and alcohols: conditions for stability and for the encapsulation of biopolymers. *Biochim. Biophys. Acta.* 1559:1–9.

24. Budin, I., R. J. Bruckner, and J. W. Szostak. 2009. Formation of protocell-like vesicles in a thermal diffusion column. *J. Am. Chem. Soc.* 131:9628–9629.

25. Bruckner, R. J., S. S. Mansy, …, J. W. Szostak. 2009. Flip-flop-induced relaxation of bending energy: implications for membrane remodeling. *Biophys. J.* 97:3113–3122.

26. Mysels, K. J., and R. J. Otter. 1961. Conductivity of mixed sodium decyl and dodecyl sulfates: the composition of mixed micelles. *J. Colloid Sci.* 16:462–473.

27. Budin, I., and J. W. Szostak. 2010. Expanding roles for diverse physical phenomena during the origin of life. *Ann. Rev. Biophys.* 39:245–263.

28. Szostak, J. W. 2011. An optimal degree of physical and chemical heterogeneity for the origin of life? *Philos. Trans. R. Soc. Lond. B Biol. Sci.* 366:2894–2901.

29. Monnard, P.-A., C. L. Apel, …, D. W. Deamer. 2002. Influence of ionic inorganic solutes on self-assembly and polymerization processes related to early forms of life: implications for a prebiotic aqueous medium. *Astrobiology.* 2:139–152.

30. Adamala, K., and J. W. Szostak. 2013. Nonenzymatic template-directed RNA synthesis inside model protocells. *Science.* 342:1098–1100.

Supporting Material

Chain-length heterogeneity allows for the assembly of fatty acid vesicles in dilute solutions

Itay Budin[1,2], Noam Prwyes[1], Na Zhang[1,3] , and Jack W. Szostak[1]

[1] Howard Hughes Medical Institute, Department of Molecular Biology and Center for Computational and Integrative Biology, Massachusetts General Hospital, 185 Cambridge St., Boston, MA 02114, USA

[2] Miller Institute for Basic Research in Science, University of California, Berkeley, 2536 Channing Way, Berkeley, CA 94720, USA

[3] High Magnetic Field Laboratory, Hefei Institutes of Physical Science, Chinese Academy of Sciences, Hefei 230031, P. R. China

This file includes Supplemental Text, Figures S1-S6, Table S1, and NMR spectra for Figure 7 and Table 1.

Derivation of the critical aggregation concentration (cac) of a multi-component mixture

We take the approach of Holland (1) to derive the cac for an ideal mixture of fatty acids. The chemical potential of species *i* as a monomer can be expressed as:

$$(1) \qquad \mu_i = \mu_i^{\circ} + RT \ln C_i^m$$

μ_i is the monomeric chemical potential of species *i*, μ_i° is its standard chemical potential, and C_i^m is the concentration of the monomer *i* in units of mole fraction in solvent (i.e. molar concentration divided by ~55). This assumes the activity coefficient of the free monomer is 1 (acts ideally), approximating free dispersal of monomers with no interactions. In a mixed aggregate,

$$(2) \qquad \mu_i^a = \mu_i^{a,\circ} + RT \ln f_i x_i$$

μ_i^a is the chemical potential of *i* in the mixed aggregate, $\mu_i^{a,\circ}$ is the chemical potential of *i* in a pure aggregate of species *i*, f_i is the activity coefficient for *i* in the aggregate (a measure of its interactions with other molecules), and x_i is the mole fraction of *i* in the mixed aggregate. For the pure aggregate of *i*, we can apply a pseudophase model, and thus:

$$(3) \qquad \mu_i^{a,\circ} = \mu_i^o + RT \ln cac_i$$

cac_i is the critical aggregation concentration (cac) for species *i* in a single-component system. At the concentration of the cac, monomers and aggregates are isoenergetic and the free energy of the monomer species is equal to that of the aggregate. Therefore,

$$(4) \qquad \mu_i^a = \mu_i$$

Substituting in Eq. 1 and 2:

$$(5) \quad \mu_i^{a,\circ} + RT \ln f_i x_i = \mu_i^{\circ} + RT \ln C_i^m$$

and Eq. 3:

$$(6) \quad \mu_i^{a} + RT \ln cac_i + RT \ln f_i x_i = \mu_i^{\circ} + RT \ln C_i^m$$

which simplifies to:

$$(7) \quad C_i^m = f_i x_i cac_i$$

If we take the case of a solution at the mixed cac (right at the formation of the first aggregates), the concentration of monomer i, C_i^m , is simply a product of its mole fraction of total lipids, X_i, and the total lipid concentration, which at that point is equal to the mixed cac (cac). Therefore,

$$(8) \quad C_i^m = X_i cac$$

Combining with Eq. 7 and rearranging:

$$(9) \quad \frac{X_i cac}{f_i cac_i} = x_i$$

The mole fractions of components i in the mixed aggregate of k components must sum to 1,

$$\sum_{i=1}^{k} x_i = 1$$

Therefore,

$$\sum_{i=1}^{k} \frac{X_i cac}{f_i cac_i} = 1 = cac \sum_{i=1}^{k} \frac{X_i}{f_i cac_i}$$

$$(10) \quad \frac{1}{cac} = \sum_{i=1}^{k} \frac{X_i}{f_i cac_i}$$

This is a general expression for the cac of a system (in total mole fraction units) with n components, each with mole fractions X_i, individual critical concentrations cac_i for their behavior

in single-component systems, and activity coefficient f_i. For micelles, fatty acids have shown ideal behavior (2), i.e. an activity coefficient of 1, thus potentially simplifying this further.

Estimation of vesicle partition of an individual species by NMR line width measurements

Because line width represents a weighted average between the species in a vesicle aggregate and as monomers (or small micelles), vesicle composition can be roughly estimated from the corresponding line widths of each component:

$$(11) \quad lw = X_m lw_m + X_a lw_a$$

Where lw is the measured line width of the sample, X_m the monomer fraction, lw_m the line width for a pure monomer sample, X_a is the aggregate (vesicle) fraction, and lw_a is the line width for a pure vesicle aggregate fraction. This is a simplification of actual fatty acid systems, which feature a ternary mixture of monomers, vesicles, and micelles (3). However, micelle samples prepared either at high pH (>10) or in the presence of detergent (Triton X-100) featured similar line widths (~2 Hz) to those of monomeric samples (i.e., those below the cac) and therefore these two states can be grouped together. A more significant assumption is that each of these states features a characteristic line width, regardless of concentration or their chemical environment. This is obviously a crude approximation, but we can test it against the line width vs. concentration data for 1-^{13}C decanoic acid from Fig. 7. We expect two regimes of line width: 1) below the cac, $lw = lw_m$, since $X_m = 1$ and 2) above the cac,

$$(12) \quad lw = X_m lw_m + X_a lw_a = \left(\frac{cac}{c}\right) lw_m + \left(1 - \frac{cac}{c}\right) lw_a$$

We set cac to 40 mM, as measured by turbidity and pinacyanol, lw_m to 2 Hz and performed a least squares fit of Eqn. 12 on the data for c > 40 mM to solve for lw_a (Fig. S6). This yielded a

reasonable fit (R^2 = 0.96) for the concentrations tested with a value for lw_a of ~130 Hz . In the case of pure oleic acid, which features a very low cac compared to the concentrations needed for NMR measurements, line width was independent of concentration under tested conditions (> 5 mM) at ~200 Hz, though fitting of Lorentzian functions to such broad peaks is a challenge. We, however, expect the value for lw_a to be intrinsically lower for decanoic acid, due to the abundance of coexisting micelles (which feature narrow peaks) characteristic of short-chain fatty acid vesicle solutions in these concentration ranges (3, 4).

While an approximation, a constant lw_a allows for the vesicle partition factor to be calculated from measured line widths. Setting the sum of X_m and X_a to 1, we can simplify Eq. 11:

$$X_a = \frac{lw - lw_m}{lw_a - lw_m} \quad (13)$$

Using the values above for decanoic acid, estimated partition coefficients were calculated for the systems and are shown in Table S1. While these partitions are dependent on a extrapolated value for lw_a (130 Hz, in this case), their relative values are not (e.g. at 50 mM vs. 15 mM). If we assume that the oleic acid features a very high aggregation partition (e.g. X_a of 1), we can further deduce vesicle compositions from these partition coefficients.

Supporting References

1. Holland, P.M. and D.N. Rubingh. 1983. Nonideal multicomponent mixed micelle model. *J. Phys. Chem.* 87:1984-1990.
2. Shinoda, K. 1954. The Critical Micelle Concentration of Soap Mixtures (Two-Component Mixture). *J. Phys. Chem.* 58:541-544.
3. Budin, I., A. Debnath, and J.W. Szostak. 2012. Concentration-driven growth of model protocell membranes. *J. Am. Chem. Soc.* 134:20812-20819.

4. Dejanović, B., K. Mirosavljević, …, P. Walde. 2008. An ESR characterization of micelles and vesicles formed in aqueous decanoic acid/sodium decanoate systems using different spin labels. *Chem. Phys. Lipids.* 156:17-25.

Supporting Figures

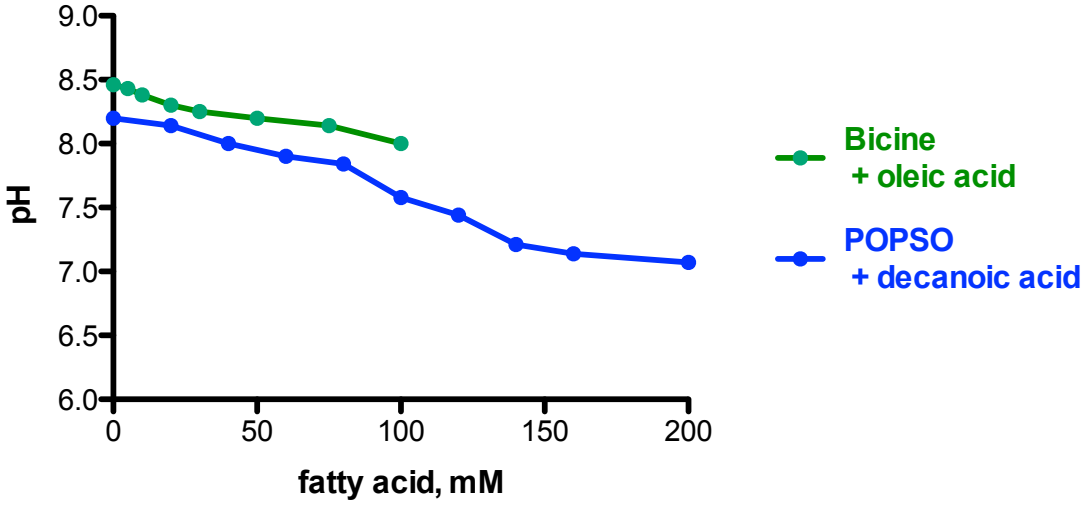

FIGURE S1 Effect of fatty acid concentration on the pH of buffered solutions used. The pH was measured of solutions of decanoic acid in 0.1 M POPSO (titrated to pH 8.2 with NaOH) and oleic acid in 0.2 M Bicine (titrated to pH 8.5 with NaOH). Connecting lines added for clarity. Samples were prepared at 30 °C and measurements taken at 23 °C.

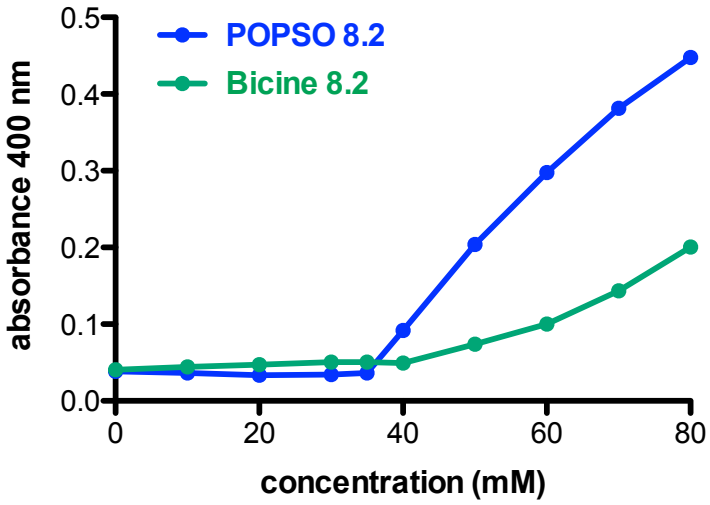

FIGURE S2 Effect of buffer used on decanoic acid vesicle assembly. POPSO and Bicine buffers, both titrated to pH 8.2 with NaOH, support decanoic acid vesicles in solutions above the cac (~40 mM in both cases). The POPSO buffers supports more abundant and/or larger vesicles, as indicated by the higher turbidity of the solution. Connecting lines added for clarity. Experiments were performed at 30 °C.

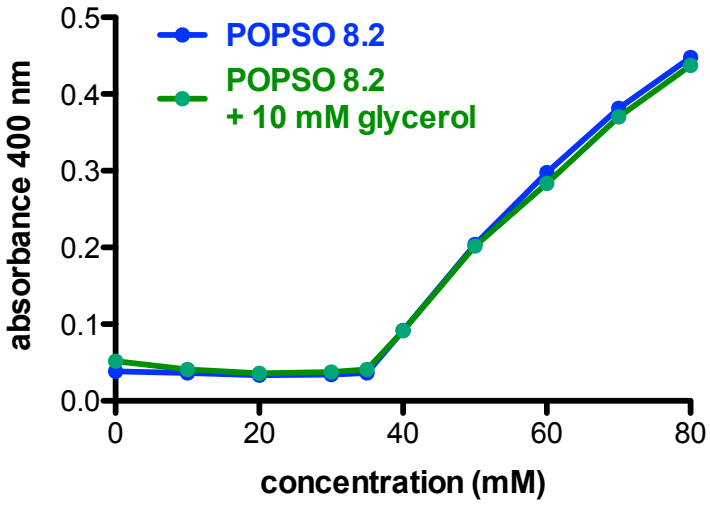

FIGURE S3 Effect of glycerol on decanoic acid vesicle assembly. The concentration of glycerol (10 mM) included in NMR experiments as an internal standard does not noticeable affect decanoic acid vesicle assembly as assayed by solution turbidity. Connecting lines added for clarity. Experiments were performed at 30 °C.

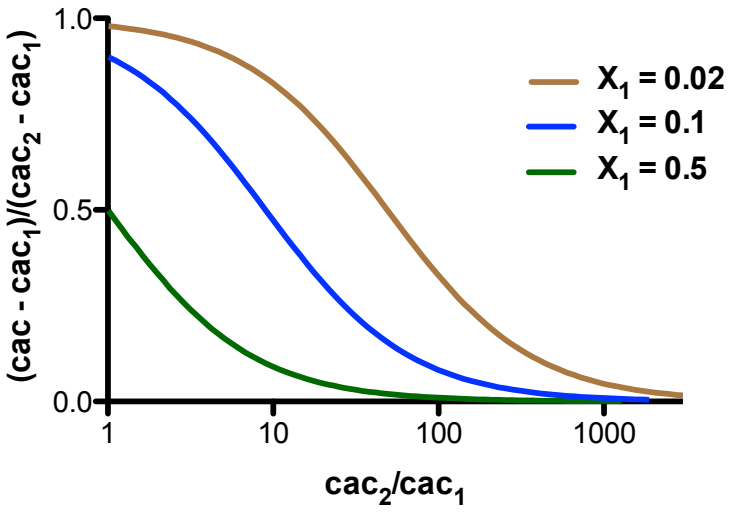

FIGURE S4 Predicted mixed cac values of a binary mixture (cac) converge to that of the longer chain species (cac_1) as the ratio of the two individual cacs (cac_2/cac_1) becomes large. Values were calculated from Eq. 4 for different mixture stoichiometries (X_1, the mole fraction of component 1). A cac_2/cac_1 ratio of 1000 corresponds to a difference of 8 carbons in the chain length of two fatty acid components.

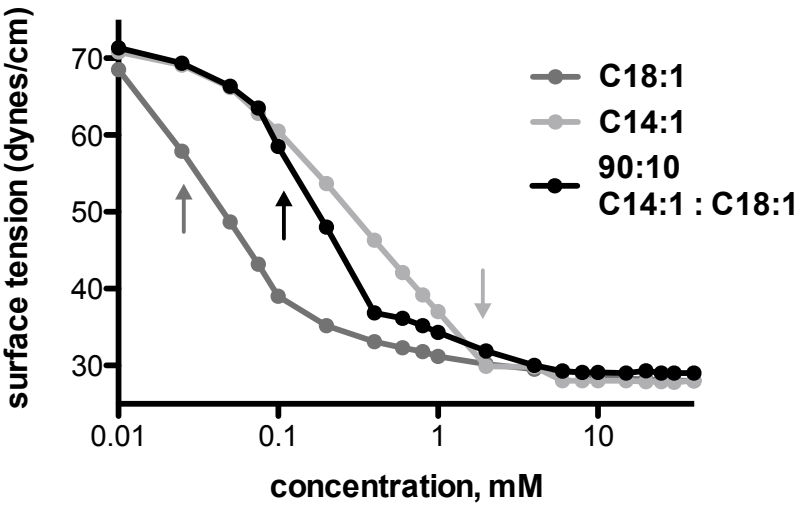

FIGURE S5 Surface tension of fatty acid solutions from Figure 2. Surface tension was measured from serial dilutions of myristoleic acid (C14:1), oleic acid (C18:1), and a 90:10 mixture of myristoleic acid : oleic acid. Surface tension decreases with increasing lipid concentration due to the ability of the amphiphilic monomers to lower the air-water interfacial energy. The decrease in surface tension plateaus due to the assembly of aggregates (vesicles or micelles), which do not interact with the interface. Arrows show the concentration at which vesicle assembly is detected using light scattering experiments shown in Figure 2. Because these concentrations are lower or equal to the concentration at which surface tension plateaus, we conclude that there is not a second, micelle critical concentration below the vesicle cac. In our model, fatty acid solutions feature only a single cac, with the structural composition of the resulting aggregate phase (i.e. vesicle vs. monomer) is dependent on solution pH. Experiments were performed at room temperature in Bicine buffer, pH 8.5.

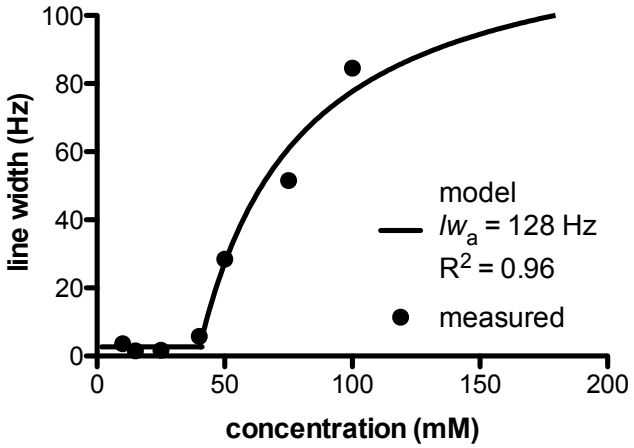

FIGURE S6 Weighted average model for 1-^{13}C decanoic acid line widths. Data from concentrations less than the cac (40 mM) were modeled as a constant line width (2 Hz); for concentrations greater than the cac, line widths were fit with a least squares regression of Eqn. 12.

Fatty acid mixture	15 mM decanoic acid	50 mM decanoic acid	15 mM 95:5 decanoic acid: oleic acid	50 mM 95:5 decanoic acid: oleic acid	15 mM 50:50 decanoic acid: oleic acid
^{13}C decanoic acid line width	1.6 Hz	28.6 Hz	14.2 Hz	49.1 Hz	36.3Hz
Estimated partition coefficient of decanoic acid into vesicles	0	0.21	0.10	0.38	0.28

TABLE S1 Estimated partition coefficients of decanoic acid into pure or mixed vesicles as extrapolated from 1-^{13}C decanoic acid line widths. Experiments were performed in POPSO buffer at 30 °C.

1D ^{13}Carbon NMR spectra for Figure 7 and Table 1

Main spectra intensities are normalized to the 10 mM glycerol standard at 72 ppm.
Inserts show a 4 ppm region at the fatty acid peak (184 or 181 ppm) and the fitted line width.

A

10 mM 1-^{13}C decanoic acid

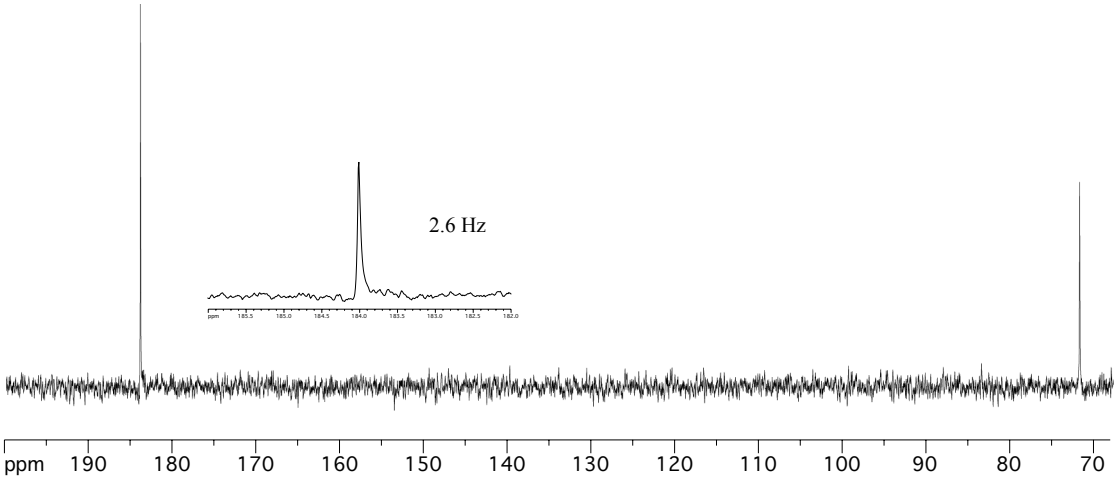

25 mM 1-^{13}C decanoic acid

B

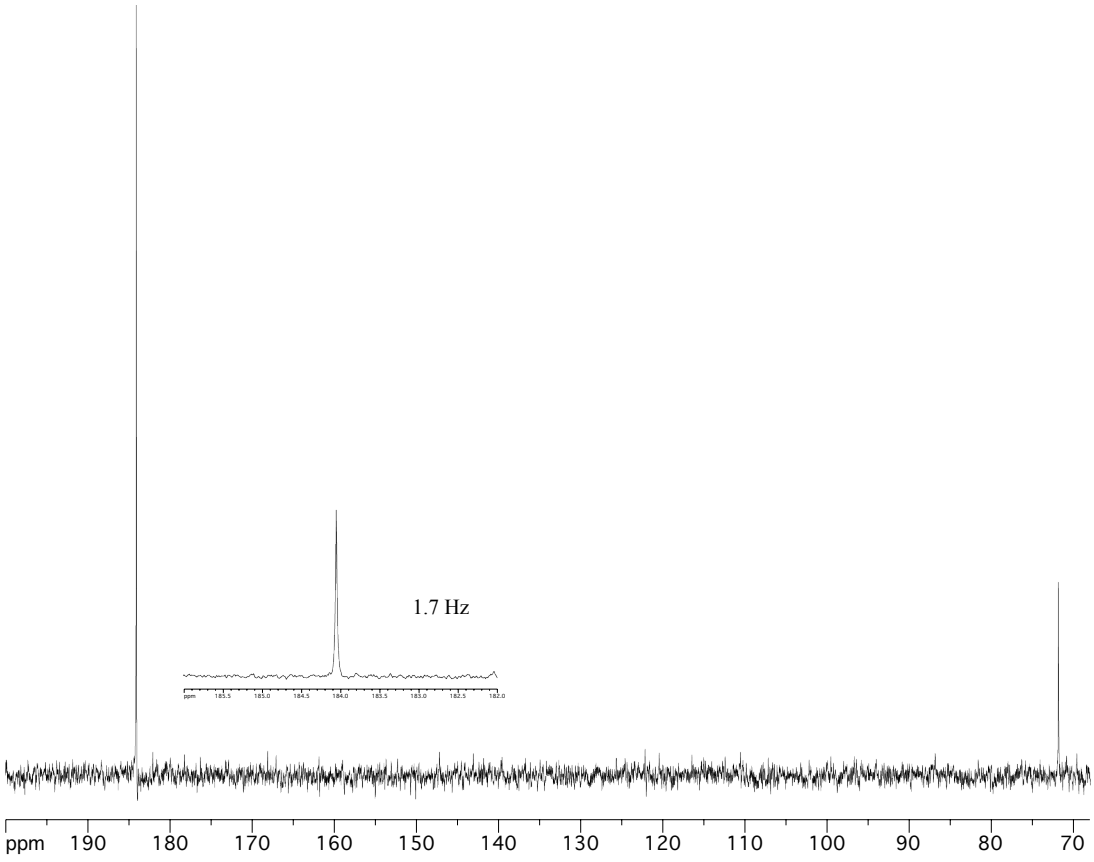

40 mM 1-^{13}C decanoic acid

C

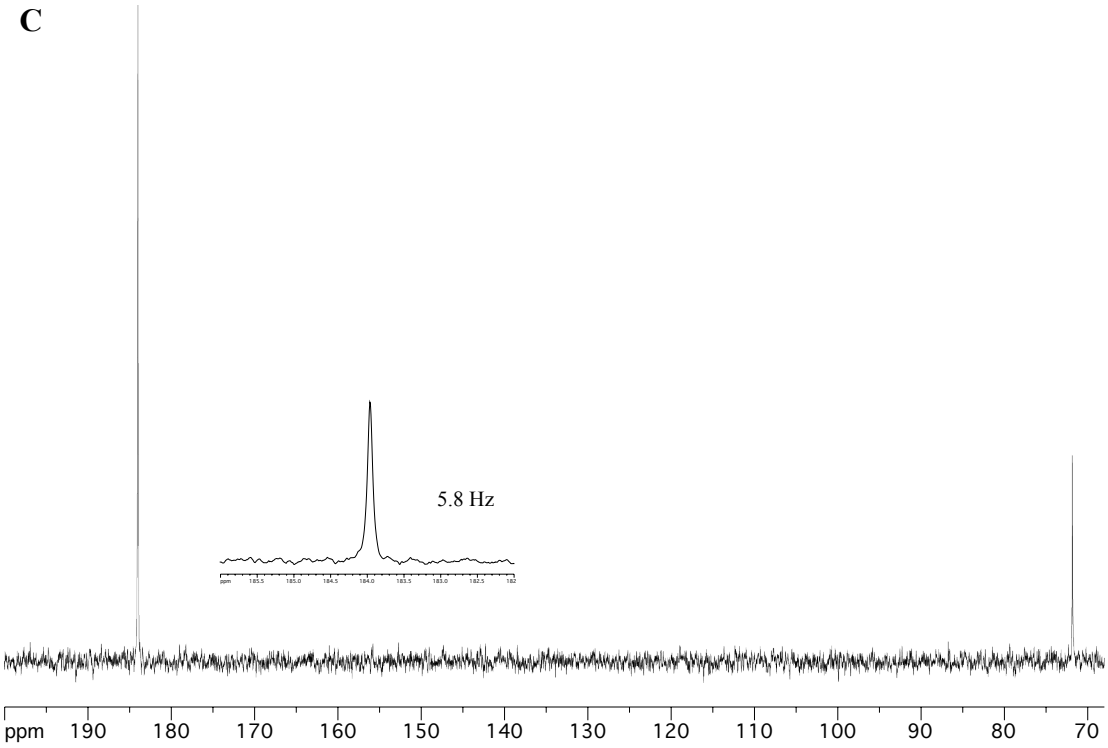

50 mM 1-^{13}C decanoic acid

D

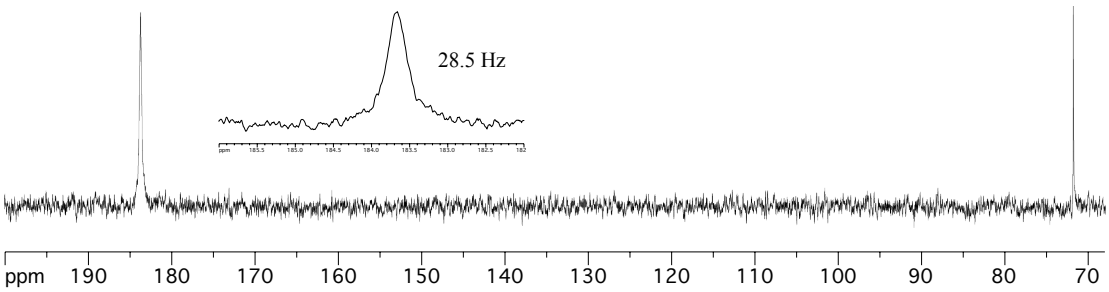

75 mM 1-^{13}C decanoic acid

E

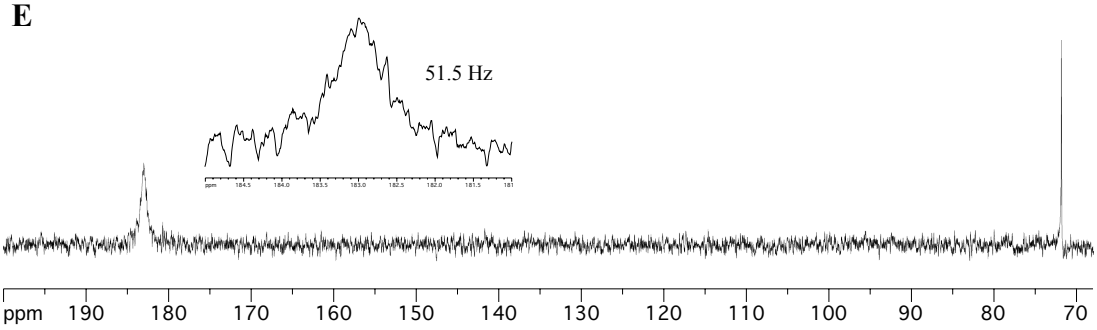

100 mM 1-^{13}C decanoic acid

F

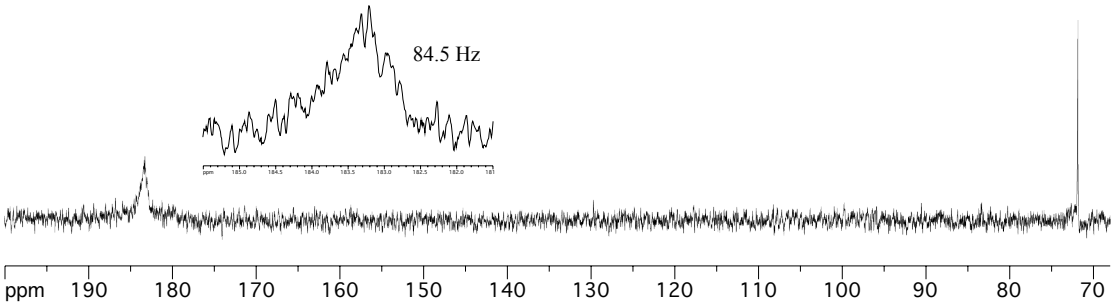

100 mM 1-^{13}C decanoic acid, pH 10

(vertical scale = 0.25x)

G

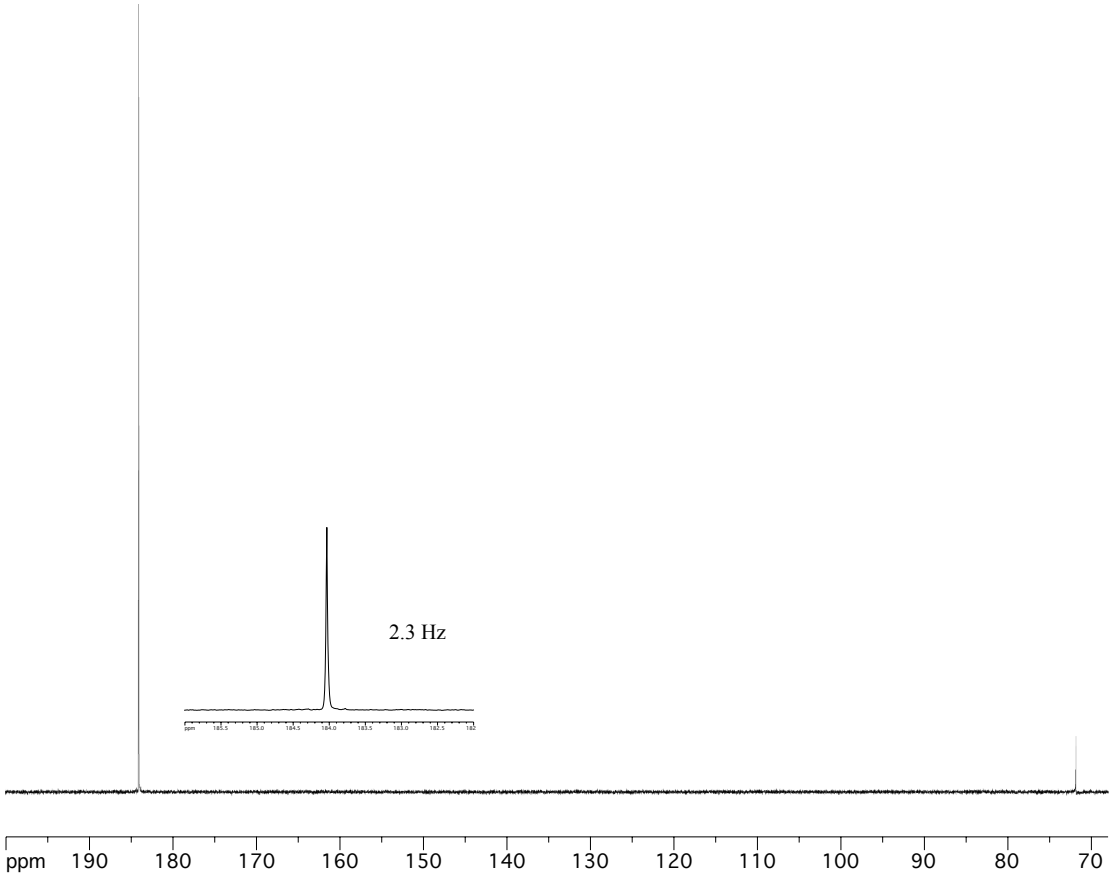

15 mM 1-^{13}C decanoic acid

H

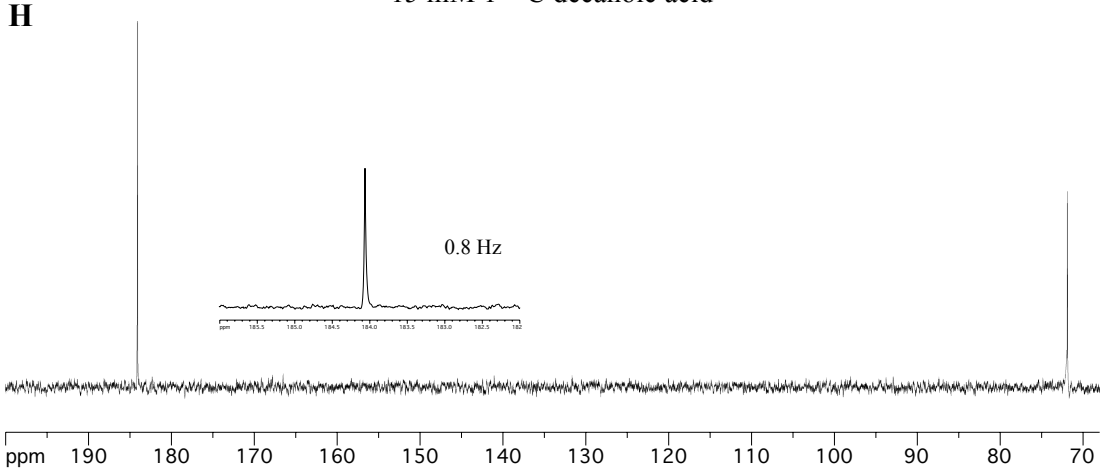

15 mM 95:5 1-^{13}C decanoic acid : oleic acid

I

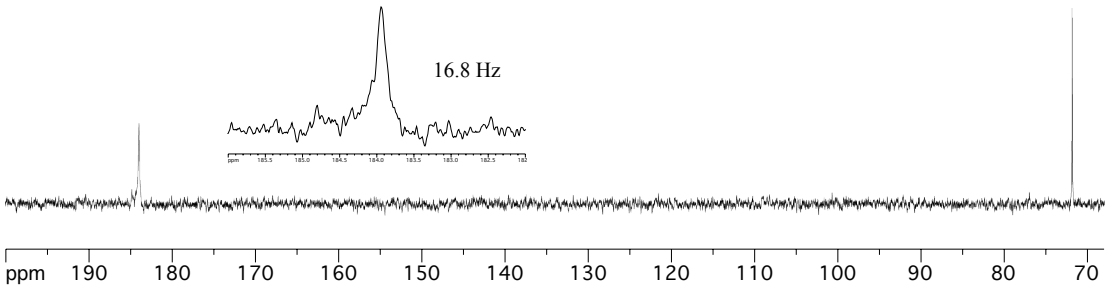

15 mM 50:50 1-^{13}C decanoic acid : oleic acid

J

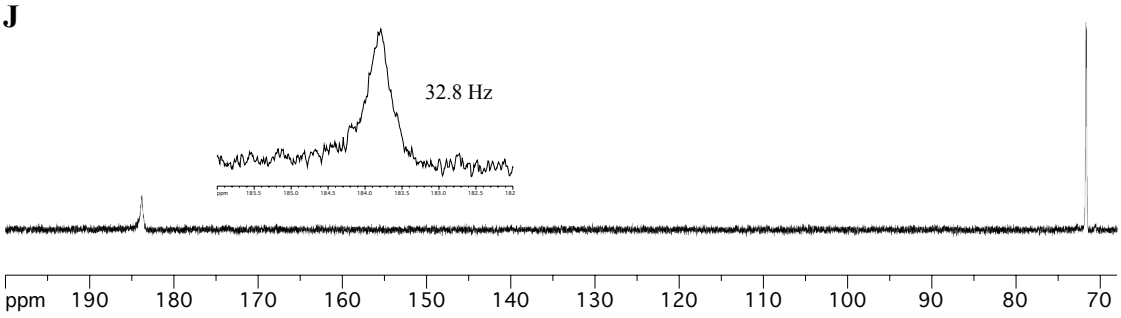

50 mM 95:5 1-^{13}C decanoic acid : oleic acid

K

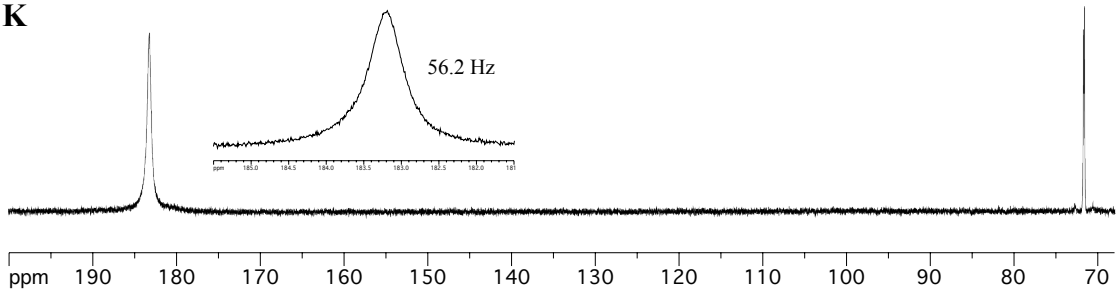

L

15 mM 1-^{13}C oleic acid

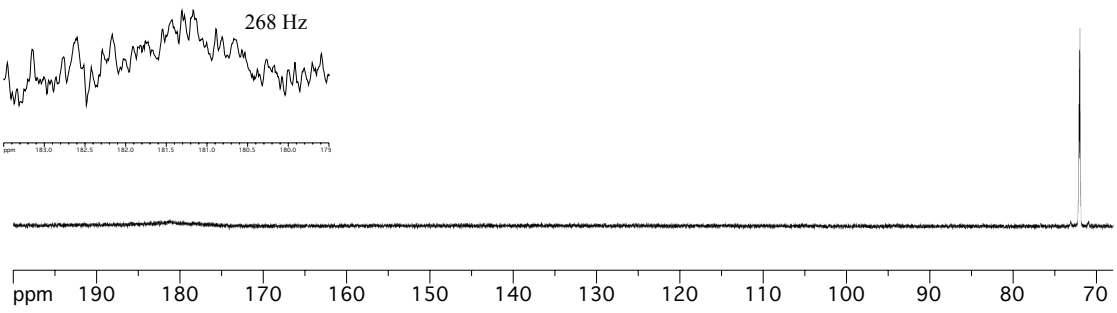

50 mM 1-^{13}C oleic acid

M

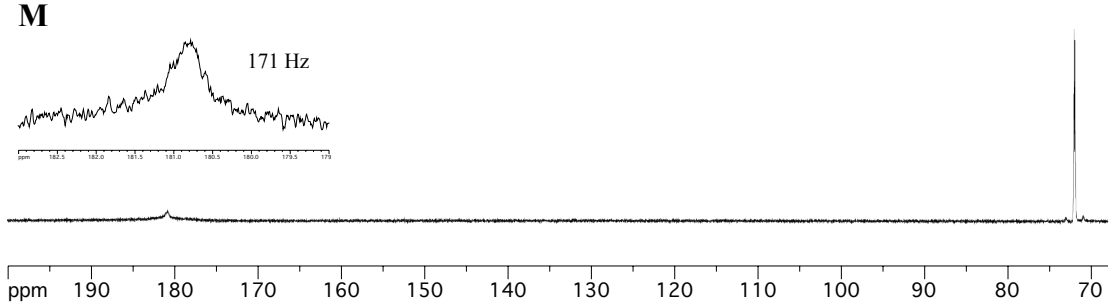

15 mM 95:5 decanoic acid : 1-^{13}C oleic acid

N

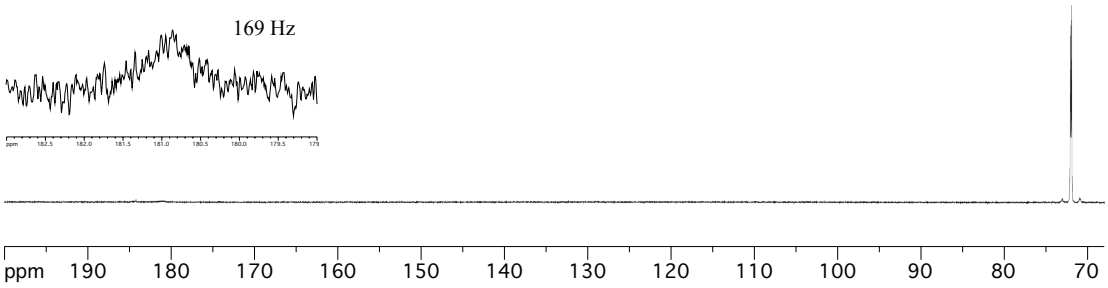

50 mM 95:5 decanoic acid : 1-^{13}C oleic acid

O

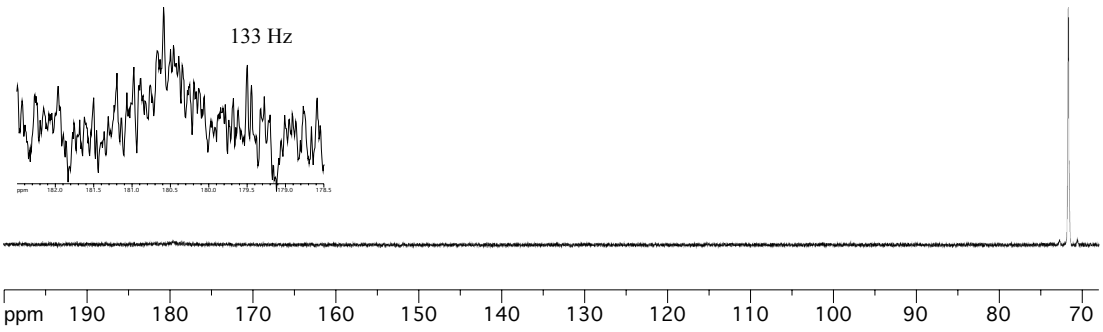

15 mM 50:50 decanoic acid : 1-^{13}C oleic acid